

Communication

Prospects for the (Hyper)Nuclei Study in the Nica Energy Range

Viktar Kireyeu, Vadim Kolesnikov, Alexander Zinchenko, Veronika Vasendina and Alexander Mudrokh

Special Issue

Selected Papers from "Physics Performance Studies at FAIR and NICA"

Edited by

Prof. Dr. Peter Senger, Prof. Dr. Arkadiy Taranenko and Prof. Dr. Ilya Selyuzhenkov



<https://doi.org/10.3390/particles6010021>



Communication

Prospects for the (Hyper)Nuclei Study in the Nica Energy Range

Viktor Kireyeu *, Vadim Kolesnikov, Alexander Zinchenko, Veronika Vasendina and Alexander Mudrokh

Joint Institute for Nuclear Research, Joliot-Curie 6, Dubna 141980, Russia
* Correspondence: vkireyeu@jinr.ru

Abstract: The production of nuclei and hypernuclei is of interest for experimental and theoretical studies: it is a big question how such weakly bound objects survive in a hot, dense environment and which new insights on the heavy-ion collisions dynamics they can bring us. We present the results on the hypernuclei feasibility study for the flagship Nuclotron-based Ion Collider fAcility (NICA)/Multi-Purpose Detector (MPD) experiment at the Joint Institute for Nuclear Research (JINR) in Dubna using the Parton-Hadron-Quantum-Molecular Dynamics (PHQMD) transport approach and a realistic reconstruction chain.

Keywords: nuclei; hypernuclei; heavy-ion; MPD; NICA; PHQMD

1. Introduction

Recent results from the experiments at the Relativistic Heavy Ion Collider (RHIC) and the Large Hadron Collider (LHC) have shown the presence of light nuclei and hypernuclei in the central rapidity region even at extremely high energies (up to several TeV) [1,2]. These observations raised the question of how such loosely coupled objects with the binding energy of several MeV can survive at high surrounding temperatures of about 100 MeV. Moreover, although the nucleon–nucleon interactions already have been studied well, the hyperon–nucleon and the hyperon–hyperon interactions are understood quite poorly. The knowledge of hyperon–nucleon potentials is of great importance for nuclear physics and astrophysics. Thus, the study of the nuclei and hypernuclei produced in heavy-ion collisions can provide new data for theoretical models.

One of the key points of the physics program at the new accelerator complex Nuclotron-based Ion Collider fAcility (NICA) constructed at the Joint Institute for Nuclear Research (JINR) [3] in Dubna is the study of the production of hyperons and hypernuclei. In this study, we use the Parton-Hadron-Quantum-Molecular Dynamics (PHQMD) [4] transport approach and the realistic detector reconstruction chain to investigate the possibility of studying hypernuclei in the Multi-Purpose Detector (MPD) experiment.

2. The Multi-Purpose Detector

The MPD (Figure 1) is designed as a spectrometer to provide large acceptance measurements of the particle production in heavy-ion collisions at the NICA accelerator complex. The Time Projection Chamber (TPC) as the main tracking device measures the momentum of the charged particles by their curvatures in the magnetic field (within $|\eta| < 1.5$ region) and their ionization energy loss (dE/dx) in the TPC gas mixture (90% argon and 10% methane). The time-of-flight (TOF) system, which is located just behind the TPC, is composed of Multi-gap Resistive Plate Chambers (MRPC) and has the time resolution of about 80 ps. The TOF system will be used together with the TPC for the identification of charged particles at momenta up to several GeV/c. The Electromagnetic Calorimeter (ECal) is situated behind the TOF system, it consists of 38,000 lead and scintillator modules coupled in a way that the longitudinal axis of each module is directed to the center of the detector (projective geometry). The ECal is dedicated to the detection of electrons and photons. An array of quartz Cherenkov counters—the Fast Forward Detector (FFD)—should provide



Citation: Kireyeu, V.; Kolesnikov, V.; Zinchenko, A.; Vasendina, V.; Mudrokh, A. Prospects for the (Hyper)Nuclei Study in the Nica Energy Range. *Particles* **2023**, *6*, 399–404. <https://doi.org/10.3390/particles6010021>

Academic Editor: Armen Sedrakian

Received: 27 January 2023

Revised: 26 February 2023

Accepted: 27 February 2023

Published: 2 March 2023



Copyright: © 2023 by the authors. Licensee MDPI, Basel, Switzerland. This article is an open access article distributed under the terms and conditions of the Creative Commons Attribution (CC BY) license (<https://creativecommons.org/licenses/by/4.0/>).

the start signal for the TOF system and for the triggering. Two arms of the Forward Hadron Calorimeter (FHCal) comprising 44 lead–scintillator modules of sampling calorimeters cover the pseudorapidity region of $2.8 < |\eta| < 4.5$ to measure the forward energy of the spectators for the event plane reconstruction and centrality determination.

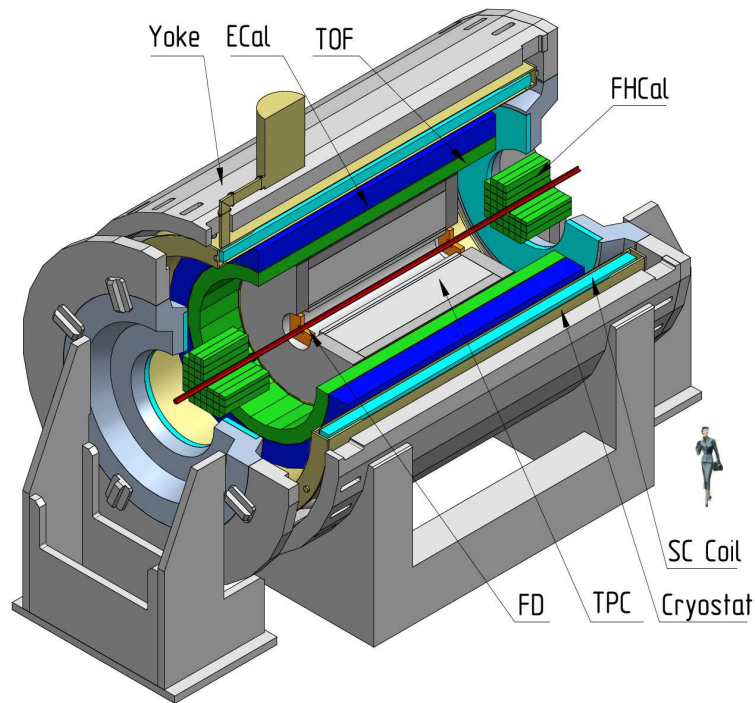


Figure 1. Schematic view of the first stage of the MPD detector.

All detector subsystems are located inside the superconducting solenoid which generates the magnetic field with the heterogeneity level below 10^{-3} and the strength up to 0.6 T. A more detailed description of the detector and its subsystems can be found in [5].

3. The Parton-Hadron-Quantum-Molecular Dynamics (PHQMD) Approach

The PHQMD [4] is a self-consistent microscopic transport approach which includes Quantum-Molecular Dynamics (QMD) for the initialization and propagation of baryons and the dynamical cluster formation, propagation of partons and mesons, as well as the collision integral from the Parton-Hadron-String Dynamics (PHSD) approach [6,7] and two algorithms for the identification of dynamically formed (hyper)nuclei: the minimum spanning tree (MST) procedure and the simulated annealing clusterization algorithm (SACA).

The dynamical cluster formation in the PHQMD is the consequence of the nucleon-nucleon interactions occurring during the heavy-ion collision evolution. The cooperation of the hadron collisions and attractive potential interactions (at baryonic densities around or below normal nuclear matter density) leads to the cluster formation. This process does not occur just at a given time or at the end of reaction, but is continuous due to the interactions between baryons, and in PHQMD we can apply the cluster recognition algorithms at several time steps.

In the present study, we used the MST procedure for the light nuclei recognition, and the algorithm is as follows: (1) two baryons are considered as a cluster if the distance between them r_{clust} is less than 4 fm; (2) another particle can be added to the cluster already found in the previous step if this particle fulfills the same condition $r_{clust} < 4$ fm with at least one particle of the cluster. Although the MST procedure is rather simple, it is very well known for a remarkably good identification of the light clusters for the decades, due to the fact that clusters with a high relative momentum are most likely not in the same place at the end of the reaction [8].

Figure 2 shows the rapidity spectra of light nuclei (d and ^3He) produced in the central $\text{Pb}+\text{Pb}$ collisions at $\sqrt{s_{\text{NN}}} = 8.8 \text{ GeV}$: the PHQMD predictions with MST algorithm (blue diamonds) agree with the NA49 Collaboration experimental data (black circles) [9] in the whole measured rapidity range.

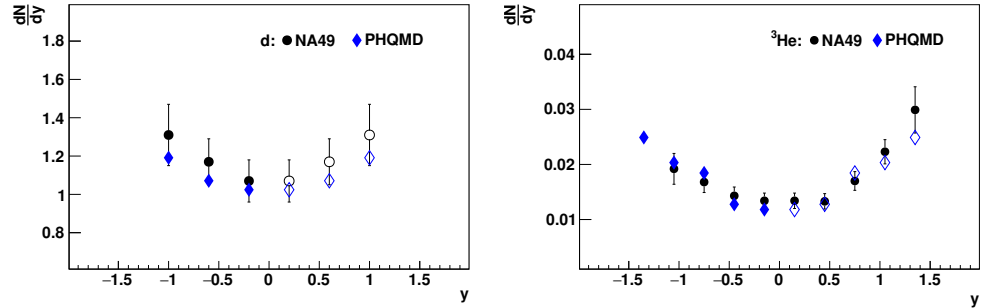


Figure 2. Rapidity spectra of deuterons and ^3He in the central $\text{Pb}+\text{Pb}$ collisions. Experimental data (black circles) are taken from NA49 Collaboration [9].

The transverse momentum distributions for both light nuclei species (d and ^3He) are displayed in Figure 3. It is clearly visible that in the whole p_T range, where NA49 Collaboration experimental data are available, the PHQMD transport approach reproduces transverse momentum spectra in different rapidity bins remarkably well.

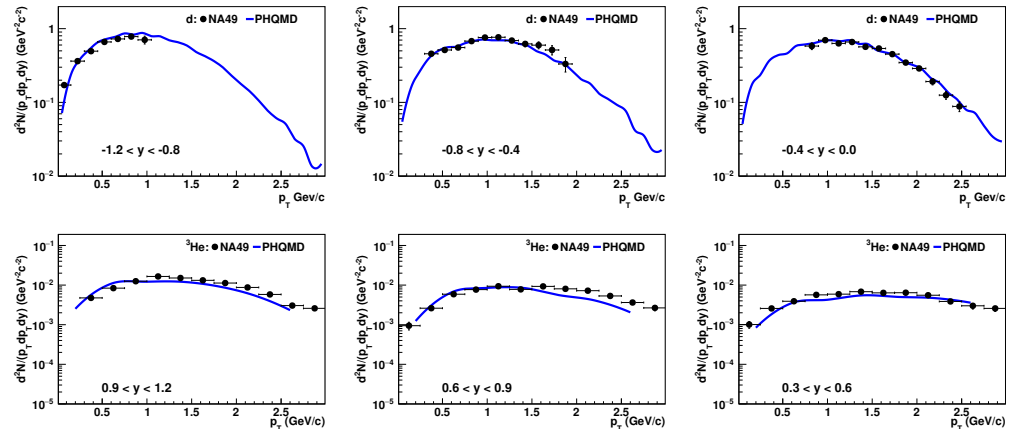


Figure 3. Transverse momentum spectra of deuterons and ^3He in selected rapidity bins for the central $\text{Pb}+\text{Pb}$ collisions. Experimental data (black circles) are taken from NA49 Collaboration [9].

Taking into account the reasonable description of the available experimental data for the light nuclei production, the PHQMD approach with the MST cluster recognition algorithm was also used as the input for our MPD hypernuclei feasibility study.

4. Results of the Hypertriton Reconstruction in the MPD Detector

For the hypernuclei production study, we used a data set of $4 \cdot 10^7 \text{ Bi} + \text{Bi}$ collisions at $\sqrt{s_{\text{NN}}} = 9.2 \text{ GeV}$ from the PHQMD event generator. The generated particles are passed through the MPD detector material within the MPDRoot [10] framework using the GEANT4 package. All the Monte-Carlo hits were digitized into signals with the realistic detector response simulation. The momentum and the trajectories of the charged particles were reconstructed using the Kalman filter technique, a subset of these trajectories was used to determine the primary vertex—the position of the interaction point. Then, all the reconstructed TPC tracks were extrapolated to the TOF detector and matched with TOF hits. In our study, we used the TPC energy loss (dE/dx) information combined with the time-of-flight information from the TOF system for the identification of charged particles. The

charged tracks are required to have at least 20 hits in the TPC volume to ensure the optimal momentum resolution and good energy loss measurements. To reduce the background from secondary particles, we selected tracks with a distance to the primary vertex of less than 3 cm. The track candidates are also required to be within the 3σ region based on the expectation from the Bethe–Bloch equation and the nominal m^2 value for the dE/dx and TOF measurements, respectively.

Hypertritons in the MPD detector were reconstructed via two decay channels: the two-body decay mode (${}^3\Lambda H \rightarrow {}^3He + \pi^-$) and the three-prong decay channel (${}^3\Lambda H \rightarrow d + p + \pi^-$). Once the daughter particles were identified, a decay vertex was found and the invariant mass was calculated. Several topological cuts have been applied to improve the purity of the signal. These cuts involve the distance of closest approach (DCA) between the particle tracks at the decay vertex, the DCA value for the reconstructed hypertriton candidate to the primary vertex, the cosine of the angle between the direction from the primary to secondary vertex and the hypertriton momentum vector, and the decay length from the event vertex to the decay point.

As an example, an invariant mass spectrum of $({}^3He, \pi^-)$ pairs is shown in the left panel of Figure 4. The right panel of the same figure indicates the results of reconstruction for the three-prong decay mode $({}^3\Lambda H \rightarrow d + p + \pi^-)$. The shown distributions are sums of the signal pairs and those from the combinatorial background (i.e., from uncorrelated combinations of candidate particles). Thus, the distributions were fitted to a combined fit function: a Gaussian for the signal and a polynomial for the background. The resulting fit functions are shown in Figure 4 by red lines and the extracted parameters for the signal (i.e., its mean and sigma) are also shown. The analysis was performed in transverse momentum bins of 0.5 GeV/c and the raw yield of hypertritons in every p_t interval was obtained as the sum of histogram counts within the region $\pm 3\sigma$ around the peak position. The background estimated as the integral of the background function under the peak area was subtracted from the signal counts. The signal should then be corrected by the efficiency due to the detector acceptance and applied selection criteria.

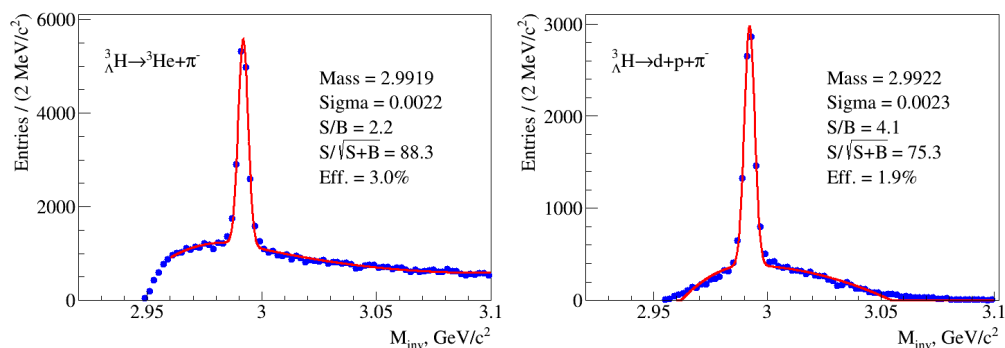


Figure 4. Left panel: invariant mass spectrum of $({}^3He, \pi^-)$ pairs in Bi+Bi collisions at $\sqrt{s_{NN}} = 9.2$ GeV . Right panel: the same for (d, p, π^-) candidates. Reconstructed data are shown by symbols and red line indicates a fit to a Gaussian plus polynomial.

Figure 5 (left panel) shows the hypertriton reconstruction efficiency for the two-body decay mode as a function of transverse momentum. The right panel of the same figure indicates the reconstructed transverse momentum spectrum of hypertritons from Bi + Bi collisions (red symbols). The comparison of the initial distribution (blue squares) and the reconstructed one indicates a good quality of the reconstruction procedure.

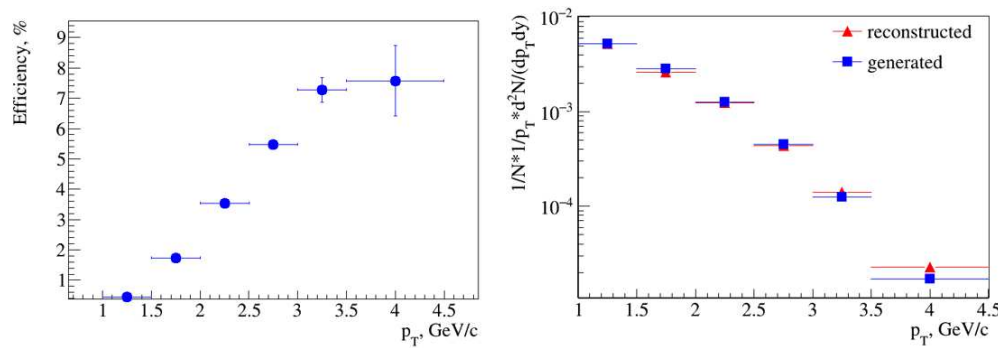


Figure 5. Left panel: efficiency of hypertriton reconstruction in transverse momentum intervals. Right panel: invariant transverse momentum spectra of hypertritons from Bi+Bi collisions. The reconstructed one is plotted by red symbols, the initial one from the model is shown by blue squares.

Finally, with the present assessment of the MPD detector performance to the reconstruction of hypertritons, we are able to estimate the expected rate of hypertriton events during the first period of data taking at NICA. Taking the NICA collider luminosity during the commissioning stage of $10^{25} c^{-1} cm^{-2}$ and assuming the PHQMD model predictions for the yields of hypernuclei as well as the overall MPD detector efficiency obtained from the current feasibility study, we expect the signal of roughly 1000 hypertritons to be registered during one week of data taking.

5. Conclusions

In this paper, the results of the MPD detector feasibility study for the hypertriton reconstruction in Bi+Bi collisions at NICA energies are presented. The PHQMD model, which can describe the overall evolution of a heavy ion collision including (hyper)cluster formation, was used as an input for the simulation. Event analysis procedure and track selection criteria were developed, which allow the extraction of the hypertriton signal in high multiplicity heavy-ion collisions. The efficiency of the MPD detector for the reconstruction of hypertritons is obtained and rough estimates of the registered hypertriton statistics during the first period of data taking at NICA are given.

Author Contributions: All the authors contributed equally to this work. All authors have read and agreed to the published version of the manuscript.

Funding: This research received no external funding.

Institutional Review Board Statement: Not applicable.

Informed Consent Statement: Not applicable.

Data Availability Statement: Not applicable.

Acknowledgments: The authors acknowledge the inspiring discussions and the theoretical support of Joerg Aichelin and Elena Bratkovskaya.

Conflicts of Interest: The authors declare no conflict of interest.

References

1. Adam, J.; Milosevic, J.; Garcia-Solis, E.J.; Calvo Villar, E.; Majka, R.D.; Weber, S.G.; Ducroux, L. $^3\Lambda$ H and $^3\bar{\Lambda}$ production in Pb-Pb collisions at $\sqrt{s_{NN}} = 2.76$ TeV. *Phys. Lett. B* **2016**, *754*, 360–372. [[CrossRef](#)]
2. Adam, J.; Adamová, D.; Aggarwal, M.M.; Rinella, G.A.; Agnello, M.; Agrawal, N.; Ahammed, Z.; Ahmed, I.; Ahn, S.U.; Aimo, I.; et al. Production of light nuclei and anti-nuclei in pp and Pb-Pb collisions at energies available at the CERN Large Hadron Collider. *Phys. Rev. C* **2016**, *93*, 024917. [[CrossRef](#)]
3. Golovatyuk, V.; Kekelidze, V.; Kolesnikov, V.; Rogachevsky, O.; Sorin, A. The Multi-Purpose Detector (MPD) of the collider experiment. *Eur. Phys. J. A* **2016**, *52*, 212. [[CrossRef](#)]

4. Aichelin, J.; Bratkovskaya, E.; Le Fèvre, A.; Kireyeu, V.; Kolesnikov, V.; Leifels, Y.; Voronyuk, V.; Coci, G. Parton-hadron-quantum-molecular dynamics: A novel microscopic n -body transport approach for heavy-ion collisions, dynamical cluster formation, and hypernuclei production. *Phys. Rev. C* **2020**, *101*, 044905. [[CrossRef](#)]
5. Abraamyan, K.U.; Afanasiev, S.V.; Alfeev, V.S.; Anfimov, N.; Arkhipkin, D.; Aslanyan, P.Z.; Zulkarneeva, Y.R. The MPD detector at the NICA heavy-ion collider at JINR. *Nucl. Instrum. Meth. A* **2011**, *628*, 99–102. [[CrossRef](#)]
6. Cassing, W.; Bratkovskaya, E.L. Parton transport and hadronization from the dynamical quasiparticle point of view. *Phys. Rev. C* **2008**, *78*, 034919. [[CrossRef](#)]
7. Cassing, W.; Bratkovskaya, E.L. Parton-Hadron-String Dynamics: An off-shell transport approach for relativistic energies. *Nucl. Phys. A* **2009**, *831*, 215–242. [[CrossRef](#)]
8. Kireyeu, V. Cluster dynamics studied with the phase-space Minimum Spanning Tree approach. *Phys. Rev. C* **2021**, *103*, 054905. [[CrossRef](#)]
9. Anticic, T.; Baatar, B.; Bartke, J.; Beck, H.; Betev, L.; Białkowska, H.; NA49 Collaboration. Production of deuterium, tritium, and He3 in central Pb + Pb collisions at 20A, 30A, 40A, 80A, and 158A GeV at the CERN Super Proton Synchrotron. *Phys. Rev. C* **2016**, *94*, 044906. [[CrossRef](#)]
10. Rogachevsky, O.V.; Bychkov, A.V.; Krylov, A.V.; Krylov, V.A.; Moshkin, A.A.; Voronyuk, V.V. Software Development and Computing for the MPD Experiment. *Phys. Part. Nucl.* **2021**, *52*, 817–820. [[CrossRef](#)]

Disclaimer/Publisher's Note: The statements, opinions and data contained in all publications are solely those of the individual author(s) and contributor(s) and not of MDPI and/or the editor(s). MDPI and/or the editor(s) disclaim responsibility for any injury to people or property resulting from any ideas, methods, instructions or products referred to in the content.